Simulation Study on Effects of Chemically Eroded Methane and Ethylene Molecules on Carbon Impurity Transport and Net Erosion of Carbon Materials

KAWAKAMI Retsuo

Faculty of Engineering, The University of Tokushima, Tokushima 770-8506, Japan

（Received: 4 October 2004 / Accepted: 24 May 2005）

Abstract

Effects of chemically eroded CD_4 and C_2D_4 molecules on local transport of ionized C impurities and net erosion of the C target are studied using a simulation code for plasma surface interactions. The calculated C^{1+} emission profile reproduces the experimental one, which indicates a stronger contribution of CD_4. For C^{2+} and C^{3+}, the contribution of C_2D_4 is stronger near the target. For their penetrations, however, the contribution of CD_4 is essential. For a high density and low temperature plasma, there is a significant influence of the charge transfer reactions of C_xD_y with D^+, by which the penetrations as well as the net erosion rates for CD_4 and C_2D_4 are suppressed with their local redeposition. The net erosion rate for C_2D_4 is higher if $Y_{CD4} = Y_{C2D4}$. If the temperature becomes high, however, the rate for C_2D_4 is suppressed by its local redeposition, and approaches that for CD_4.

1. Introduction

Because of a high thermal shock resistance, C material will be used as a plasma facing material of ITER divertor target plates. However, there is a crucial issue in net erosion relevant to the divertor lifetime, namely, chemical sputtering of C material. This causes penetration of hydrocarbons, such as methane (CD_4) and ethylene (C_2D_4), to the core plasma [1]. The impurity penetration contaminates the plasma, which results in a degradation of the plasma performance. Thus, effects of the chemically eroded CD_4 and C_2D_4 molecules on the impurity penetration and the net erosion rate need to be clear to improve the plasma performance and the divertor lifetime.

In this study, the effects on the penetrations of ionized C impurities are studied using a simulation code for plasma surface interactions, ERIm [2]. The result is compared with experimental data [3]. Also, the effects on the net erosion rates for a variety of plasma parameters and for the normal ITER divertor plasma predicted by B2-EIRENE [4] are studied. The paper discusses how the penetration depth from the C target to the core plasma and its net erosion rate are changed by chemical erosion (release) of CD_4 and C_2D_4 each.

2. Simulation code and model

On the basis of the Monte-Carlo impurity transport model [5] and the binary collision model [6], ERIm simulates the penetration depth of ionized C impurities from a C target exposed to the plasma/impurity ions and its net erosion rate. Only the important features of the code for this study are described here (see ref. [2] for details). For the penetration depth, the eroded impurities are assumed to be subject to the Lorentz and friction forces [5]. The impurity ionization, dissociation, and recombination dissociation reactions with e^- and the charge transfer reactions with D^+ are included in this code. The reaction chain by which CD_4 changes to C^+ is given as the rate coefficients by Ehrhardt *et al*. [7]. For C_2D_4 to C^+, the rate coefficients by Brooks *et al*. are used [8], and for C^0 to C^{3+}, those by Lennon are used [9]. The simulation is continued until the impurities are locally redeposited on the targets or leave the computational domain. For simplicity, the sticking coefficient is assumed to be 100％：all of the hydrocarbons locally returned back to the target by the friction force are redeposited. For the net erosion rate, the gross erosion/deposition by the ions impinging on the target and the local redeposition of the eroded hydrocarbons (as described above) are taken into account

Corresponding author's e-mail: retsuo@ee.tokushima-u.ac.jp

[6]. Here, a word "deposition" is used for impurities transported by a plasma from other wall targets, and "redeposition" is used for those locally returned back to the target. The energy of the impinging ions is given by the Maxwellian distribution with an acceleration energy due to the electrostatic sheath potential, $V_S = T_e/2 \ln 2\pi(m_e/m_i)(1 + T_i/T_e)$, and the flux is given by $n_i(T_i + T_e)/m_i^{1/2}$ [10]. Here, T_e and T_i are the plasma electron and ion temperatures in front of the target, respectively, m_e and m_i are the electron and ion masses, respectively, and n_i is the ion density. CD_4 and C_2D_4 molecules are assumed to be released from the C target according to their chemical release yields, Y_{CD4} and Y_{C2D4}, respectively. For the physically released C^0 atoms, their release is based on the binary collision model [5]. In this study, there are no differences in chemical properties between the deposited layer and the bulk target.

3. Results and discussion

3.1 Carbon impurity transport

The simulation of the penetration depth is performed based on the TEXTOR-94 edge plasma [11]. The electron density and temperature profiles used in this study are the exponential functions fitted to those measured by the Li- and He-diagnostics. They are given by $n_e(r) = n_{eLCFS} \exp -(r - 0.46\,\text{m})/0.02\,\text{m}$ and $T_e(r) = T_{eLCFS} \exp -(r - 0.46\,\text{m})/0.025\,\text{m}$, where n_{eLCFS} (= 10^{18} m^{-3}) and T_{eLCFS} (= 30 eV) are the density and temperature at the last closed flux surface (LCFS), at a minor radius of $r \sim 0.46$ m, respectively [3,12]. For the impinging ions, D^+ (~ 98 %) and C^{4+} (~ 2 %) are used assuming $T_i = T_e$ [12].

The radial penetrations of C^{1+}, C^{2+} and C^{3+} generated through the reaction chains of CD_4, C_2D_4 and C^0 released from the target at $r = 0.47$ m are simulated as shown in Fig. 1. In the result, $Y_{CD_4} = 3.6$ % and $Y_{C2D4} = 0.9$ % are assumed, which are based on the experimental data for C targets exposed to the TEXTOR-94 plasma [11] and 200 eV D^+ beam [1]. As shown in Fig. 1(a), the C^{1+} penetration is in good agreement with the measured CII light emission profile [3] (this means that their decay lengths are the same). The agreement indicates that the contribution of CD_4 is stronger than that of C_2D_4 near the target. For C^{2+} and C^{3+}, however, the opposite results occur as shown in Figs. 1(b) and 1(c), which indicate the stronger contribution of C_2D_4 near the target. However, the contribution of CD_4 is found to be essential for the penetration of highly ionized C impurities under the low density and high temperature plasma ($n_{eLCFS} = 10^{18}$ m^{-3} and $T_{eLCFS} = 30$ eV).
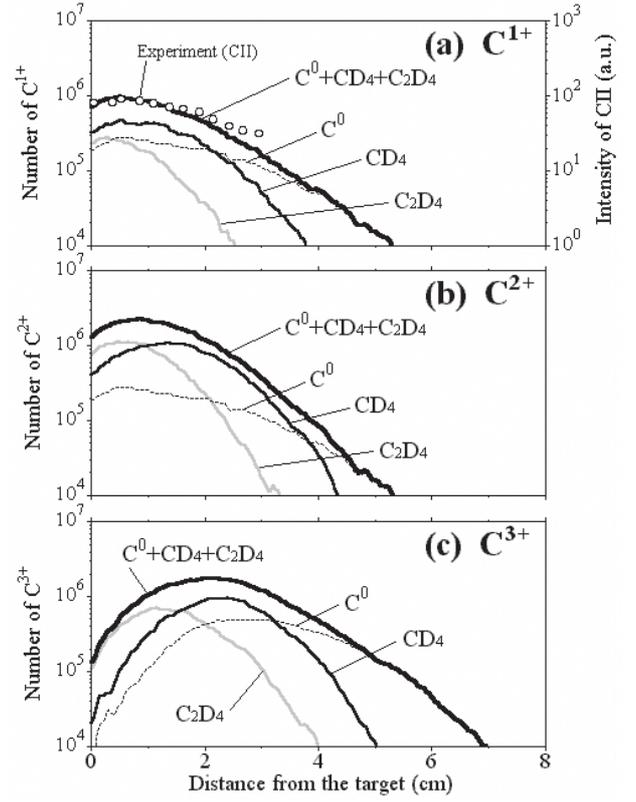

Fig. 1 Radial penetrations of C^{1+}, C^{2+} and C^{3+} generated through the reaction chains of CD_4, C_2D_4 and C^0 released from a C target exposed to a D^+ plasma including C^{4+} impurity ($n_{eLCFS} = 10^{18}$ m^{-3}, $T_{eLCFS} = 30$ eV). Open circles indicate the measured CII emission profile [3].

If the density is higher and the temperature is lower ($n_{eLCFS} = 10^{19}$ m^{-3} and $T_{eLCFS} = 3$ eV), there is a significant influence of the charge transfer reactions of C_xD_y with D^+ as shown in Fig. 2 (for the low density plasma, there is no influence). By the charge transfer reactions, there is a suppression in the total number of C^{1+} and C^{2+} penetrating to the core plasma [compare Fig. 2(a) with Fig. 2(c), and compare Fig. 2(b) with Fig. 2(d)]. In particular, for CD_4, it is more pronounced. For C_2D_4, there is no significant suppression, because the released C_2D_4 molecule tends to be locally redeposited before it changes to C^{1+} or C^{2+}. Thus, since the contributions of CD_4 and C_2D_4 are almost the same as shown in Figs. 2(c) and 2(d), they are found to play an important role in both the C^{1+} and C^{2+} penetrations under the high density and low temperature plasma. Incidentally, there is no contribution of C^0 to these C impurity penetrations, because the exposure ion energy is lower than a threshold energy below which the physical release never occurs [13].
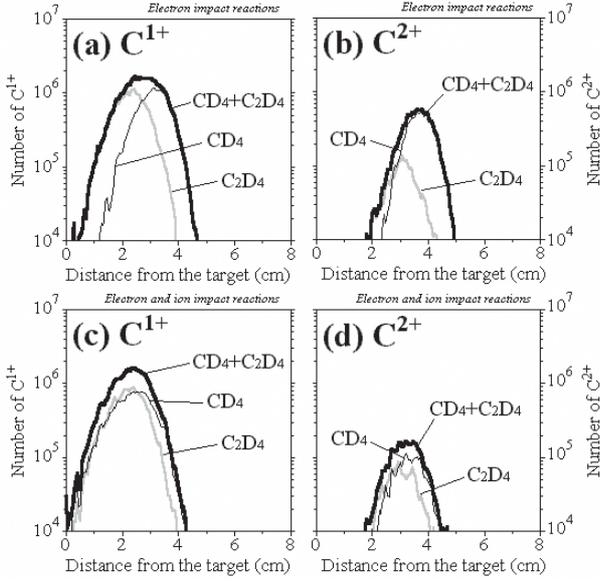
Fig. 2 Comparison in the C^{1+} and C^{2+} penetrations between the reaction chain of CD_4 and C_2D_4 with e^-, (a) and (b), and that with e^- plus D^+, (c) and (d), under a high density and low temperature plasma ($n_{eLCFS} = 10^{19}$ m^{-3}, $T_{eLCFS} = 3$ eV).

3.2 Net erosion of carbon material

The simulation of the net erosion rate (including the redeposition rate) for different plasma densities and temperatures is also performed based on the same TEXTOR-94 edge plasma as described in the previous subsection [11] (contribution of physical sputtering is included in this result). In order to clarify a difference in the results between CD_4 and C_2D_4 chemical erosions, the same erosion yields are assumed: $Y_{CD4} = Y_{C2D4} = 4.0$ %. A change in the net erosion rate of the C target at $r = 0.47$ m with n_{eLCFS} and T_{eLCFS} is calculated as shown in Fig. 3 (if there is no chemical erosion, net deposition of the impinging C impurity occurs at a low temperature, see ref. [14] for details).

At a low density ($n_{eLCFS} = 10^{18}$ m^{-3}), there is a difference in the results between the CD_4 and C_2D_4 reaction chains with e^-. The net erosion rate for C_2D_4 is higher [Fig. 3(a)], although its redeposition rate is higher [Fig. 3(a')]. This is simply because the gross erosion for a molecule of C_2D_4 is equivalent to that for two C atoms. On the other hand, they have a similarity that they increase with T_{eLCFS} due to an increase in the physical erosion. However, if the density increases ($n_{eLCFS} = 10^{19}$ m^{-3}), there is a drastic change in the net erosion rate for C_2D_4 [Fig. 3(b)]. With increasing T_{eLCFS}, the net erosion rate for C_2D_4 increases, and then decreases at $T_{eLCFS} > 5$ eV. The further increase in T_{eLCFS}(> 40 eV) makes it increase again, but it is almost the same as that for CD_4. The drastic change is because the redeposition rate for C_2D_4 increases rapidly
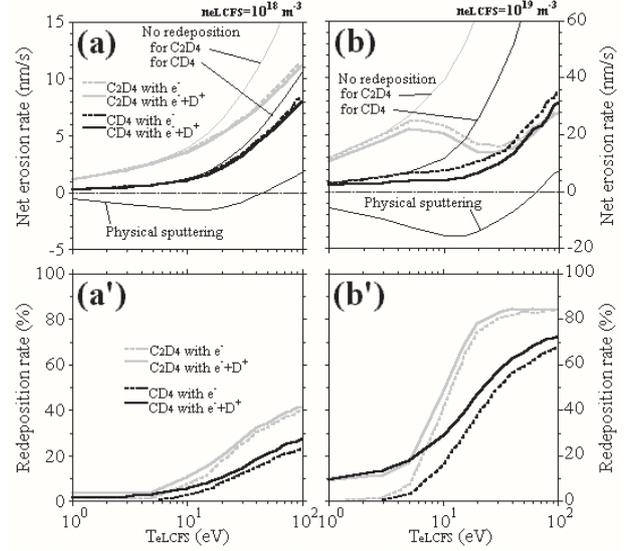

Fig. 3 Comparison in the net erosion rate, (a) and (b), and the redeposition rate, (a') and (b'), between CD_4 and C_2D_4 chemical erosions for different plasma densities and temperatures.

with T_{eLCFS} [Fig. 3(b')]. In this calculation, the redeposition comes from the friction forces on the impurity ions in the direction parallel to the magnetic field (no thermal forces are taken into account). Thus, at the high density and temperatures, the net erosion rate for C_2D_4 is found to be significantly suppressed by its local redeposition.

If the charge transfer reactions with D^+ are added (black and gray solid curves), both of the net erosion rates are suppressed at the high density [Fig. 3(b)]. Due to this addition, for example, both of the redeposition rates at $T_{eLCFS} < 5$ eV are enhanced from 0 % to 10 % [Fig. 3(b')]. On the other hand, at the low density, there is little influence of the charge transfer reactions [Figs. 3(a) and 3(a')]. Thus, at the high density plasma, the net erosion rates for CD_4 and C_2D_4 are expected to be suppressed by their strong local redeposition resulting from the charge transfer reactions.

For the normal ITER divertor plasma [4,15], the net erosion rates along the outer target plate for CD_4 and C_2D_4 are calculated assuming $Y_{CD4} = Y_{C2D4} = 1.0$ %, as shown in Fig. 4. At locations of $z <\sim 0.1$ m, i.e., at the private region and the strike point vicinity (where the density increases from 5×10^{19} m^{-3} to 2×10^{21} m^{-3} with increasing z, while the temperature keeps ~ 3 eV), the net erosion rate for C_2D_4 with e^- is higher than that for CD_4 with e^-. This indicates that, for C_2D_4, the net erosion at these plasma regions would be more serious if $Y_{CD4} = Y_{C2D4}$. In contrast, at $z >\sim 0.1$ m, i.e., at the SOL region (where the density decreases to 5×10^{18} m^{-3} with increasing z, while the temperature increases to 18
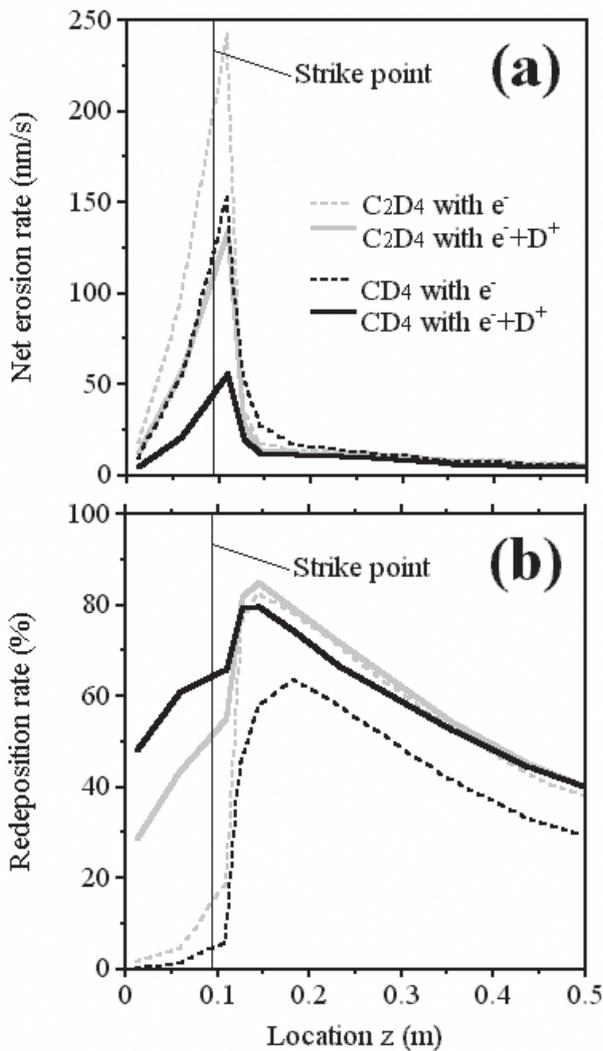
Fig. 4   Comparison in the net erosion rate (a) and the redeposition rate (b) between CD_4 and C_2D_4 chemical erosions for the ITER-FEAT divertor plasma [4,15].

eV), both are almost the same. This indicates a significant suppression of the net erosion for C_2D_4, which is attributed to the high redeposition rate for C_2D_4, as has already been described above. As expected from the result of Fig. 3, the additional charge transfer reactions brings about a significant suppression of the net erosion rates at the private region and the strike point vicinity for CD_4 and C_2D_4.

4. Conclusion

The simulated C^{1+} penetration at $n_{eLCFS} = 10^{18}$ m^{-3} and $T_{eLCFS} = 30$ eV reproduces the experimental one, which indicates that the contribution of CD_4 is stronger than that of C_2D_4. For C^{2+} and C^{3+}, however, the opposite result occurs near the target, which indicates the strong contribution of C_2D_4. For their penetrations, however, the contribution of CD_4 is essential. For a high density and low temperature plasma, there is a significant influence of the charge transfer reactions of C_xD_y with D^+, by which the penetrations are significantly suppressed. For the net erosion rate, there is also an influence of the charge transfer reactions: the net erosion rates for CD_4 and C_2D_4 are suppressed by their local redeposition. Also, the net erosion rate for C_2D_4 is higher than that for CD_4 if $Y_{CD4} = Y_{C2D4}$. However, if the temperature becomes high, the rate for C_2D_4 is suppressed by its local redeposition, and approaches that for CD_4.

References
[1]   B.V. Mech *et al.*, J. Nucl. Mater. **255**, 153 (1998).
[2]   R. Kawakami, Jpn. J. Appl. Phys. **43**, 785 (2004).
[3]   A. Kirschner *et al.*, Phys. Scr. **T91**, 57 (2001).
[4]   G. Federici *et al.*, J. Nucl. Mater. **313-316**, 11 (2003).
[5]   D. Naujoks, Nucl. Fusion **33**, 581 (1993).
[6]   W. Moller *et al.*, Comput. Phys. Commun. **51**, 355 (1988).
[7]   A.B. Ehrhardt *et al.*, Rep. Princeton Plasma Phys. Lab., PPPL-2477, 1986.
[8]   J.N. Brooks *et al.*, Rep. Argonne Natl. Lab. ANL/FPP/TM-297, 1999.
[9]   M.A. Lennon *et al.*, Rep. Culham Lab., CLM-R270, 1986.
[10]   P.C. Stangeby, *The Plasma Boundary of Magnetic Fusion Devices* (IOP Publishing, London, 2000), p. 79.
[11]   A. Pospieszczyk *et al.*, J. Nucl. Mater. **241-243**, 833 (1997).
[12]   M. Brix, Rep. IPP Julich, Jul-3638, 1998.
[13]   W. Eckstein, Rep. Max-Plank Inst. Plasmaphysik IPP9/117, Garching (1998).
[14]   T. Mitani *et al.*, J. Nucl. Mater. **329-333**, 830 (2004).
[15]   R. Kawakami *et al.*, Jpn. J. Appl. Phys. **42**, 3623 (2003).